

Laser plasma interaction physics on the LIL facility

P.-E. Masson-Laborde^{1,a}, S. Depierreux¹, D.T. Michel³, S. Hüller⁴, D. Pesme⁴, J. Robiche⁴, P. Loiseau¹, V.T. Tikhonchuk⁵, C. Stenz⁵, P. Nicolai⁵, M. Casanova¹, D. Teychenne¹, D. Marion¹, C. Goyon¹, V. Yahia², C. Riconda², N.G. Borisenko⁶, W. Nazarov⁷, R. Wrobel¹ and C. Labaune²

¹ EA, DAM, DIF, 91297 Arpajon Cedex, France

² LULI, Ecole Polytechnique, CNRS, CEA, UPMC, 91128 Palaiseau, France

³ Laboratory for Laser Energetics, Rochester, NY 14623, USA

⁴ Centre de Physique Théorique, CNRS, École Polytechnique, 91128 Palaiseau Cedex, France

⁵ CELIA, Université Bordeaux 1, 33405 Talence Cedex, France

⁶ Lebedev Physical Institute, 53 Leninskii Prospect, Moscow 119991, Russia

⁷ University of St. Andrews, Fife KY169ST, Scotland, UK

Abstract. We present an overview of the interpretation of laser plasma interaction (LPI) experiments carried out on the LIL facility. These multikilojoule experiments have been done using underdense foam targets at 0.351 μm laser light leading to high temperature and large plasmas. We discuss the interpretation using our different numerical tools: hydrodynamics simulations carried out with the code FCI2 to characterize the plasma, linear gain estimates with the postprocessor Piranah and paraxial simulations with the code HERA.

1. INTRODUCTION

In order to understand the behavior of parametric instabilities such as stimulated Brillouin scattering (SBS) or Stimulated Raman scattering (SRS) in conditions relevant to ignition plasmas [1, 2], we need some multikilojoule experiments which can lead to high temperature and large plasmas. In the past, there have been lots of experiments in low temperature plasmas (with T_e typically around 1keV) [3, 4], and many comparisons with numerical simulations [5, 6] which have shown the importance of taking into account all the physics in our numerical tools.

In order to prepare the first experiments on the National Ignition Facility (NIF) and to study in more details plasma parameters encountered in indirect drive ignition design, a series of laser-plasma interaction experiments were done on the Omega laser facility [7] and on the NIF Early Light (NEL) laser, the first quad of the NIF between 2005 and 2009. All these experiments which were done for large (multimillimeter long) and high temperature (typically between 1.5 and 3.5 keV) plasmas gave useful informations on the behavior of SBS and SRS under plasma and laser conditions close to NIF. In particular, the role of optical beam smoothing techniques such as polarization smoothing on the mitigation of filamentation and SBS/SRS has been proven during these campaigns and used for the first “full” NIF experiments done between 2009 and 2012 [8].

^ae-mail: paul-edouard.masson-laborde@cea.fr

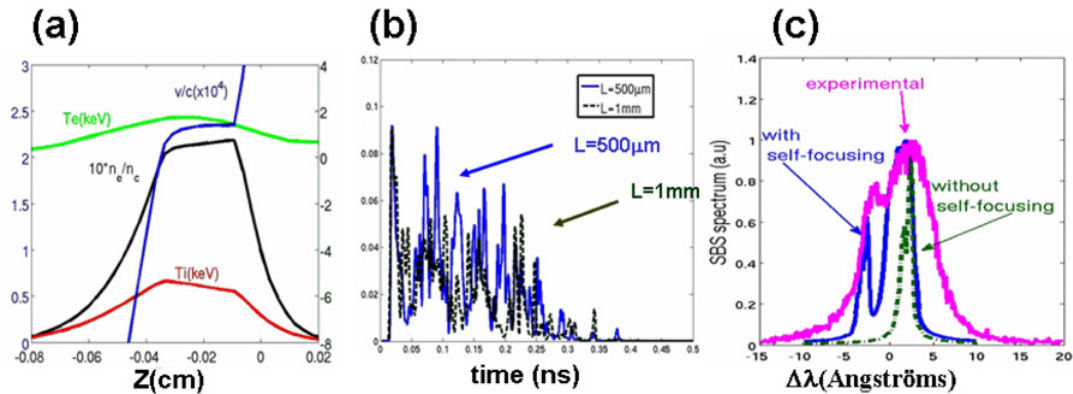


Figure 1. (a) Hydrodynamic profiles from FCI2 simulation at 500 ps for a 7 mg/cc, 500 μm foam. (b) SBS reflectivity as a function of time, for two different foam lengths, $L = 1 \text{ mm}$ and $L = 500 \mu\text{m}$ for a 7 mg/cc foam. (c) lineout of the experimental SBS spectrum, and spectrum from HERA simulations with and without self-focusing.

In order to prepare the first Laser MegaJoule (LMJ) experiments and to validate specific technical choices (such as the implementation of longitudinal smoothing by spectral dispersion (LSSD) as laser beam smoothing techniques), the same approach has to be done. This validation step needs to be carried out, as in the Omega or NEL laser facility, for large (millimeter size) and hot plasmas (typically around 2 keV) with large focal spot, which can be achieved using the LIL facility which is a prototype of a quadruplet of the LMJ. Experiments carried out with underdense foams can mimic the propagation of the laser beam along the hohlraum gas and can achieve these high temperature regimes while at the same time give the possibility to study competition between different mechanisms as SBS and SRS and plasma-induced smoothing (PIS)[9]. Such plasma conditions can also give usefull information for the study of parametric instabilities in the context of shock-ignition scheme [10].

2. THE LIL EXPERIMENTS

The LIL facility delivers around 12 kJ at 351 nm in a 2.7 ns square pulse, resulting in an average intensity on target in the range of $4 \times 10^{14} \text{ W/cm}^2$ to $8 \times 10^{14} \text{ W/cm}^2$ with a focal spot size of 700 μm diameter at best focus. Different lengths for the $\text{C}_{12}\text{H}_{16}\text{O}_8$ foams (resulting once fully ionized in $Z = 4$ and $A = 8$) have been used from 300 μm to 1 mm, and different densities between 3 and 10 mg/cc (respectively 10% and 35% of the critical density at 3ω light). The purpose of these experiments was to study the evolution of the parametric instabilities and the effect of the LSSD. Temporal smoothing is achieved on the LIL/LMJ using two modulators: the first one at 2 GHz is to avoid SBS in the optics and is always activated, and the second one at 14 GHz has been activated for part of the shots only.

3. RESULTS AND INTERPRETATION

To analyze the experimental results, the first step is to characterize the plasma, which is done using the 2D Lagrangian code FCI2. Then, from a direct analysis of the plasma profiles coming from FCI2, the postprocessor Piranah gave us the SBS/SRS spectrum and helped us to validate the hydrodynamic simulation by a direct comparison with the experimental spectrum. On a second step, the SBS evolution and laser propagation can be more correctly described using the code HERA, which describes in 2D/3D the propagation of the incident and backscattered fields, and the evolution of the ion acoustic waves (IAW) in an expanding plasma by means of the decomposition method [12]. Plasma profiles are

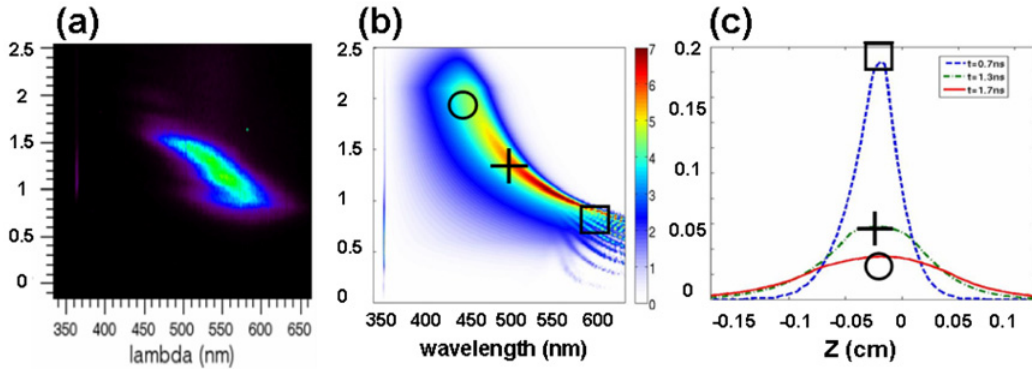


Figure 2. (a) SRS experimental spectrum and (b) computed with PIRANAH for a 7 mg/cc, 500 μm foam. (c) Lineouts of the density profile at different times. The markers show the SRS spatial activity.

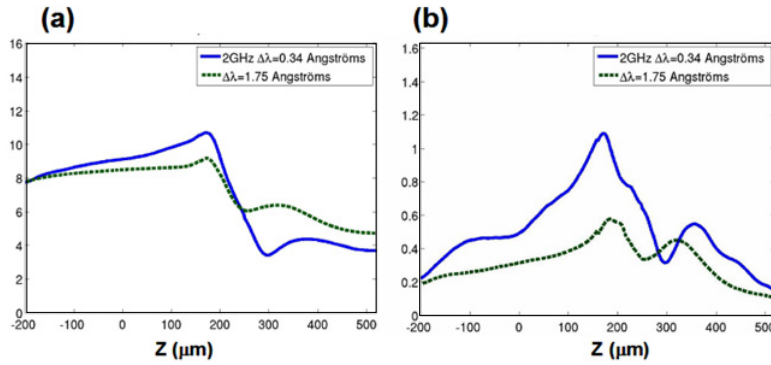


Figure 3. Fraction of hot spots (percentage) having intensity larger than (a) two times the average intensity and (b) five times the average intensity for 2 GHz and 2+14 GHz SSD, as computed with HERA.

extracted from FCI2 simulations and given as an input in HERA, which can, with a realistic description of the laser (including the smoothing technique) give us a SRS reflectivity.

Hydrodynamic simulations with FCI2, which were done with a non-local electron transport model [11], show the electron temperature of the foam can reach around 2 keV as illustrated in Fig. 1(a) showing plasma conditions obtained at the peak of the laser pulse for a 7 mg/cc, 500 μm foam. A large homogeneous plateau can be seen in the electron density when at the same time, the experimental SRS level of reflectivity is the most important. Plasma conditions given by FCI2 indicate that in these plasmas, the IAW are in a weakly damped regime, with a small level of Landau damping ($v_{iaw}/\omega_{iaw} \simeq 0.03$).

Using the 14 GHz modulator leads experimentally to a reduction of SRS by a factor 2 compared to shots with the 2 GHz modulator only. The reduction of the SRS reflectivity is directly correlated to the reduction of the very intense hot spots due to the SSD technique. As can be seen in Fig. 3, the number of hot spots having intensity larger than two times the average intensity (Fig. 3(a)) and five times the average intensity (Fig. 3(b)) is reduced when a bandwidth of 1.75 \AA (at 3ω) is used.

3.1 Stimulated Brillouin Scattering evolution

The simulated SRS spectrum from the foam obtained from Piranah is not consistent with the experimental spectrum in terms of wavelength shift but is consistent in time duration (in both cases

almost 1ns of SBS activity). While the experimental one shows a large extension between -3 and $+7\text{\AA}$ and two distinct peaks around the laser wavelength, the computed linear spectrum only shows one component around $6-7\text{\AA}$, indicating that SBS should come from the density plateau. Nevertheless, 2D paraxial simulations with HERA have confirmed that self-focusing creates very intense hot spots localized in the expanding part of the plasma, and the associated PIS reduces the contrast in the homogeneous part of the plasma. For this reason, SBS cannot grow in the homogeneous part but preferentially in the expanding part. The spectrum from HERA can reproduce the features of the experimental one as can be seen in Fig. 1(c): the same wavelength extension and two peaks on both sides of the laser wavelength, each of them associated with a different localization of the SBS activity (in the plateau and in the expanding plasma). The influence of PIS can explain the unchanged behavior of the SBS reflectivity level when the length of the foam is changed from $500\ \mu\text{m}$ to $1\ \text{mm}$, as can be seen from simulation in Fig. 1(b) and confirmed in the experiments. The plasma induced incoherence prevents SBS to grow deeper inside the plasma and localizes the IAW in the expanding part.

3.2 Stimulated Raman Scattering evolution

The experimental SRS spectrum from the $7\ \text{mg/cc}$, $500\ \mu\text{m}$ foam is illustrated in Fig. 2(a) as well as the simulated one from Piranah in Fig. 2(b). Both spectrums show a nice agreement in wavelength (between $600\ \text{nm}$ and $450\ \text{nm}$), and time duration. The position of the three markers in Fig. 2(b) can help us to localize the maximum SRS spatial activity at different times, knowing the temperature at this particular time. These markers are depicted on the simulated lineouts of the electron density in Fig. 2(c) and show that the spatial localization stays at the top of the expanding plasma. Linear gains are very small and consistent with the low level of SRS measured in the experiments ($R_{SRS} \simeq 1-2\%$). The decrease of the SRS activity in time is consistent with the decrease of the electron density, which means that in these experiments the SRS remains in the linear regime and is coming from the most intense hot spots. Using the $14\ \text{GHz}$ modulator leads experimentally to a reduction of SRS by a factor 2 compared to shots with the $2\ \text{GHz}$ modulator only. The reduction of the SRS reflectivity is directly correlated to the reduction of the very intense hot spots due to the SSD technique. As can be seen in Fig. 3, the number of hot spots having intensity larger than two times the average intensity (Fig. 3(a)) and five times the average intensity (Fig. 3(b)) is reduced when a bandwidth of $1.75\ \text{\AA}$ (at 3ω) is used.

4. CONCLUSION

The analysis conducted using our numerical tools gives us some indications on the behavior of parametric instabilities in such plasmas. The good agreement between SRS experimental and simulated spectrums indicates that the hydro-radiative simulations give consistent density and temperature conditions related to the experiments, and that SRS is probably in a linear regime, mainly dominated by the most intense hot spots. In that case, large kinetic effects able to create much more complicated physics as inflation or two dimensional effects due to electron trapping [13] are not expected to occur. The SBS behavior can only be explained by means of HERA simulations which can reproduce the IAW spatial localization. No other nonlinear effect, such as ion kinetic effects [14], need to be introduced in order to reproduce the experimental evolution of SBS in these experiments. Follow-on work is underway to understand the effect of the LSSD used on the LIL facility on the evolution of the parametric instabilities.

References

- [1] C. Cherfils *et al.*, Plasma Phys. Contr. Fus. **51**, 124018 (2009)
- [2] C. Cherfils *et al.*, J. Phys.: Conf. Ser. **244**, 022009 (2010)
- [3] C. Labaune *et al.*, J. Phys. IV **133**, 29 (2006)

- [4] C. Labaune *et al.*, European Physical Journal D **44**(2), 283 (2007)
- [5] S. Hüller *et al.*, J. Phys.: Conf. Ser. **112**, 022031 (2008)
- [6] P.-E. Masson-Laborde *et al.*, J. Phys. IV **133**, 247 (2006)
- [7] D.H Froula *et al.*, Phys. Plasmas **14**, 055705 (2007); D.H Froula *et al.*, Phys. Plasmas **17**, 056302 (2010); S.H Glenzer *et al.*, Nucl. Fusion **44**, S185–S190 (2004);
- [8] S.H. Glenzer *et al.*, Plasma Phys. Contr. Fus. **54**, 045013 (2012); D. E. Hinkel *et al.*, Phys. Plasmas **18**, 056312 (2011)
- [9] C. Labaune *et al.*, J. Phys. Conf. Ser. **244**, 022021 (2010)
- [10] S. Depierreux *et al.*, Plasma Phys. Contr. Fus. **53**, 124034 (2011)
- [11] G. P. Schurtz, Ph. D. Nicolaï, M. Busquet, Phys. Plasmas **7**, 4238 (2000)
- [12] S. Hüller *et al.*, Phys. Plasmas **13**, 022703 (2006)
- [13] P.-E. Masson-Laborde *et al.*, Phys. Plasmas **17**, 092704 (2010)
- [14] F. Detering *et al.*, J. Phys. IV France **133**, 339 (2006)